

NaOH-treated dead leaves of *Ficus racemosa* as an efficient biosorbent for Acid Blue 25 removal

S. N. Jain¹ · P. R. Gogate¹

Received: 31 May 2016/Revised: 25 August 2016/Accepted: 7 November 2016
© Islamic Azad University (IAU) 2016

Abstract A novel biosorbent synthesized from *Ficus racemosa* leaves based on the treatment using NaOH was applied for removal of Acid Blue 25 from aqueous solution. The synthesized biosorbent was characterized using scanning electron microscopy, Fourier transform infrared spectroscopy and Brunauer–Emmett–Teller analysis. NaOH treatment was demonstrated to remove lignin content from the biomass and to induce the development of significant pores. Batch experiments were performed to evaluate the effect of important operating parameters such as pH (range of 2–10), biosorbent dose (range of 1–10 g/L), contact time (range of 0–5 h), initial dye concentration (range of 50–400 mg/L) and temperature (range of 293–323 K) on the extent of removal of Acid Blue 25. The established optimum conditions were pH of 2, biosorbent dose of 4 g/L, contact time of 3 h and temperature of 323 K, yielding maximum removal of dye. Pseudo-second-order model was found to best fit the kinetic data. Langmuir and Temkin isotherm models were found to best fit the equilibrium data. The obtained thermodynamic parameters confirmed endothermic and spontaneous nature of adsorption. The study established the utility of novel biosorbent for removal of Acid Blue 25 with higher adsorption capacities (83.33 mg/g) as compared to the more commonly used adsorbents. Desorption-adsorption studies conducted for seven cycles indicated potential reusability of synthesized biosorbent for the treatment of dye effluents.

Keywords Acid Blue 25 · Adsorption kinetics · Desorption · *Ficus racemosa* · Isotherms · Thermodynamics

Introduction

Color is the most visible form in which pollution is noticed, and the main contributing factor to this type of pollution is the discharge of dyes into water from various industries such as textile, electroplating, paper, food, plastic and tanneries (Aksu et al. 2008). It is difficult to treat wastewater containing dyes since dyes are optically and thermally stable due to the complex aromatic structure (Kumar et al. 2010). Dyes offer resistance to chemical, biochemical and photochemical degradation (Saeed et al. 2015a), and hence, it is important to develop improved treatment processes. Dyes are harmful to the human and aquatic life. The presence of dyes in water imparts color to water and reduces the penetration of sunlight to the interior of the water body and causes reduction in the photosynthesis of plants affecting their growth and in general the entire aquatic life (Lee et al. 2014; Saeed et al. 2016). The pollution due to the dyes may also cause cancer and mutation in mammals (Daneshvar et al. 2014). Exposure to dyes can also result in irritation to skin, eyes (Mane and Babu 2013) and respiratory tract in human beings and animals (Saeed et al. 2015b). Considering all these negative effects, it is imperative to develop effective treatment schemes for the removal of dyes from wastewater before it can pollute the natural sources of water and create significant environmental issues.

Various methods have been applied for the treatment of dyes containing effluents, such as membrane separation (Sachdeva and Kumar 2009), oxidation (Malik and Saha 2003), ion exchange (Greluk and Hubicki 2011) and

✉ P. R. Gogate
pr.gogate@ictmumbai.edu.in

¹ Chemical Engineering Department, Institute of Chemical Technology, Nathalal Parekh Marg, Matunga, Mumbai 400019, India



coagulation (Shi et al. 2007). However, these physico-chemical processes suffer from limitations such as incomplete removal and higher costs of treatment which makes the use restricted especially by the small-scale industries and the methods cannot be applied to remove wide range of dyes from wastewater (Gupta and Suhas 2009). In a recently reported improved catalytic oxidation approach (Saeed et al. 2015a, b, 2016), degradation of dye is performed using an oxidant in the presence of a catalyst. In this approach as well, adsorption of dye occurs on the catalytic surface which is then followed by chemical reaction. Another improved approach for treatment of dye can be based on the gamma ray treatment alone, which can also be intensified using additional oxidant as H_2O_2 (Muneer et al. 2015). A possible limitation of the oxidation approaches based on the use of chemicals is that these chemicals may add to the overall pollutant load if not utilized completely in the treatment. Compared with other methods, especially oxidation-based approaches, adsorption is simple in operation and cost-effective (Yang et al. 2011). Activated carbon is widely used adsorbent which shows large adsorption capacities due to its large specific surface area (Saygılı and Güzel 2015), but at the same time suffers from limitations of high production cost and difficulty in effective regeneration and reuse. It has been reported that the use of activated carbon is not so efficient and also at times uneconomical for industrial applications (Mokri et al. 2015). These disadvantages have directed interest in developing low-cost adsorbents, especially from the industrial solid wastes, natural materials and agricultural by-products, as an alternative to commercial activated carbon (Yagub et al. 2014).

Many researchers have investigated the removal of dyes from wastewater using naturally available adsorbents such as phoenix tree leaves (Han et al. 2009), *Platanus orientalis* leaves (Peydayesh and Rahbar-Kelishami 2015), untreated low-rank coal (Janoš et al. 2007), jujuba seeds (Reddy et al. 2012), papaya seeds (Pavan et al. 2014), bagasse fly ash (Mane et al. 2007), grapefruit peel (Saeed et al. 2010) etc. Many researchers have also attempted to improve the activity of the adsorbents for intensified removal of dyes based on the chemical treatments using $ZnCl_2$ (Angin 2014), $Ca(PO_3)_2$ (Tovar-Gómez et al. 2012), H_3PO_4 (Benadjemia et al. 2011), NaOH (Lin et al. 2013), surfactant (Zhao et al. 2014), oxalic acid (Gong et al. 2008), HCl (Toor et al. 2015), etc. A detailed literature survey revealed that utilization of dead (fallen) tree leaves has not been explored so far for the development of adsorbents and subsequent application for the removal of Acid Blue 25 (AB 25) from wastewater, which falls under the second most important class of commercial dyes as anthraquinonic dyes. AB 25 was chosen as a model anthraquinonic dye due to its significant applications in

different processing sectors such as nylon, wool, ink and paper (Duman et al. 2011) and possible presence in the effluents creating environmental concerns. The present work has thus focused on the synthesis of biosorbent from dead leaves of *Ficus racemosa* (FR) considered as sustainable source, and also the effect of activation using NaOH treatment has been investigated. The objective is to obtain improved biosorbent from waste biomass, which can give higher adsorption capacities for the removal of AB 25 from wastewater. The effects of pH, biosorbent dose, contact time, initial AB 25 concentration and temperature on the extent of adsorption have been investigated. Kinetic and thermodynamic studies were also performed to establish the mechanism and nature of adsorption of AB 25 on synthesized biosorbent. The entire research work has been performed at K.K. Wagh College of Engineering, Nashik, India, with characterization studies at Institute of Chemical Technology, Mumbai, India.

Materials and methods

Biosorbent synthesis and characterization

Dead leaves of FR were collected from Nashik, Maharashtra, India. Leaves were washed with distilled water to remove dust and impurities present on the surface and then dried in sunlight to evaporate the residual moisture. Leaves were then crushed in a grinder and sieved to get the desired particle size. The obtained FR leaves powder was treated with 1% (by weight) NaOH solution in the ratio of 1:5 (powder/NaOH, weight/volume) and kept in oven at 323 K for 4 h so that lignin-based content of leaves could be removed. The FR powder was subsequently filtered, washed with distilled water and activated in hot air oven at 353 K for 24 h. The synthesized NaOH-treated FR (NTFR) biosorbent was placed in airtight container for use in the further study.

Surface characteristics and morphological features of NTFR biosorbent were investigated by scanning electron microscope (SEM, JEOL-6380, USA). The functional groups responsible for adsorption of AB 25 on NTFR biosorbent were characterized using the Fourier transform infrared spectroscopy (FTIR, PerkinElmer Spectrum BX, USA). FTIR spectra of NTFR biosorbent before and after adsorption were recorded over a range of $400\text{--}4000\text{ cm}^{-1}$ at room temperature (298 K) using KBr pellet. Brunauer–Emmett–Teller (PMI BET Sorptometer-201AEL-20SEL, USA) analysis was used to determine specific surface area, pore volume and pore diameter of the NTFR biosorbent.

The point of zero charge (pH_{pzc}) was determined based on the pH measurements. pH_{pzc} is the value of pH at which adsorbent surface has net zero charge. Solid addition method was employed to determine the pH_{pzc} (Unuabonah



et al. 2009). A set of 50 mL each of 0.1 M KCl solutions were prepared with initial pH (pH_i) in the range of 2–12 (interval of 1 each) by adding either 0.1 N HCl or 0.1 N NaOH as required. No color changes of the dye solutions were observed when pH was varied from 2 to 12. In each solution, 0.15 g of NTFR adsorbent was added and the mixtures were agitated in orbital shaker for 24 h at room temperature. The final pH (pH_f) of each solution was noted. The difference (ΔpH) between pH_i and pH_f was calculated, and the point where ΔpH value was zero is established as the pH_{pzc} .

Pollutant investigated in the work

Acid Blue 25 dye (CI 62,065, molecular formula = $C_{20}H_{13}N_2NaO_5S$, molecular weight = 416.38 g/mol) has been selected as the pollutant in the present study and was obtained from Sigma-Aldrich, Mumbai, as analytical grade compound. The physical appearance of the dye was a dark blue powder. The obtained dye was used without further purification. Stock solution of 1000 mg/L of dye was prepared by dissolving dye in double-distilled water. The solutions of required concentrations were then prepared by diluting the stock solution with distilled water.

Analysis of dye

Calibration curve was prepared by measuring absorbance at different concentrations of AB 25 at λ_{max} of 602 nm using UV–visible Spectrophotometer (UV 1800, Shimadzu, Japan). The concentration of AB 25 in the withdrawn solutions was then determined using the calibration curve and measurements of absorbance.

Experimental methodology

Different sets of batch adsorption experiments were conducted to study the efficacy of dye removal from aqueous solution as a function of operating parameters by varying pH, biosorbent dose, contact time, initial dye concentration and temperature. The experiments were performed by taking 50 mL of dye solution in 100 mL of stoppered conical flasks. A known amount of biosorbent was added into the dye solution and subsequently the suspension was agitated for required time in orbital shaking incubator (Bio-Technics, India) at 150 rpm, at required pH and at the desired temperature. The pH of solution was determined with pH meter (Cool pH 201, BSR Technologies, Nashik) and kept at the desired value by adding 0.1 M NaOH or 0.1 M HCl. Samples were withdrawn at appropriate time intervals and centrifuged in a research centrifuge (Remi scientific works, Mumbai) at 8000 rpm for the removal of suspended particles. Supernatant samples were analyzed to

determine the residual dye concentration. The effect of pH on dye removal was studied over the range of 2–10 at 303 K, whereas the effect of biosorbent dose was investigated over the range of 1–10 g/L at 303 K temperature and pH of 2. The effect of contact time on the extent of dye removal was studied at different initial dye concentrations of 50, 100, 150 and 200 mg/L, at constant operating conditions of 303 K temperature, pH of 2 and biosorbent dose of 4 g/L. The effect of operating temperature on the equilibrium adsorption capacity was studied at varying temperatures of 293, 303, 313 and 323 K for an initial dye concentration in the range of 50–400 mg/L (eight different initial concentrations for each temperature). Desorption studies were carried out under fixed condition of initial dye concentration of 100 mg/L and the adsorbent was used again for seven cycles. All the experiments were performed in triplicates, and average values were considered for further calculations to determine the kinetic, isotherm and thermodynamic parameters.

The amount of AB 25 dye adsorbed on NTFR biosorbent at any time t was calculated using the following equation:

$$q_t = \frac{(C_i - C_t)V}{m} \quad (1)$$

where q_t is mg of dye adsorbed per g of biosorbent at any time t (mg/g). C_i and C_t are initial concentration and concentration of dye at any time t , respectively (mg/L). V is volume of dye solution (L), and m is amount of biosorbent used (g).

Results and discussion

Characterization of biosorbent

Images obtained from the scanning electron microscopy analysis of NTFR biosorbent before and after the adsorption studies are shown in Fig. 1. SEM image of the biosorbent before adsorption (Fig. 1a) shows that the surface of NTFR biosorbent is fibrous and rough and consists of significant number of pores which are ideal characteristics for the efficient adsorption of AB 25 dye. These pores are large enough to allow the dye molecules to diffuse into the lignocellulosic structure allowing efficient adsorption on the active sites. The SEM image (Fig. 1b) after adsorption clearly shows that AB 25 dye has diffused into the pores and adhered on the biosorbent surface. The FTIR analysis results for the NTFR biosorbent before and after adsorption of dye are shown in Fig. 2a, b, respectively. The broad and strong peak around 3444 cm^{-1} is attributed to the O–H groups of cellulose which gets shifted after adsorption to 3464 cm^{-1} indicating the interaction between O–H group of biosorbent and –N– functional group of AB 25. The peak at 2925 cm^{-1} is attributed to the C–H stretching, whereas the strong peak at 1622 cm^{-1} is



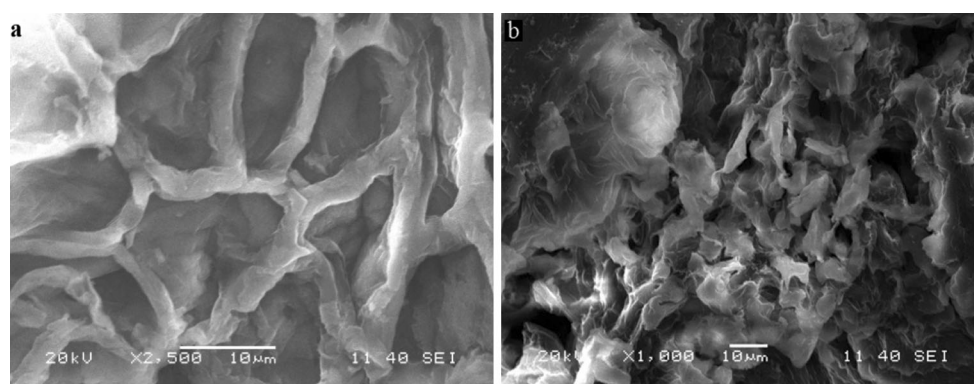
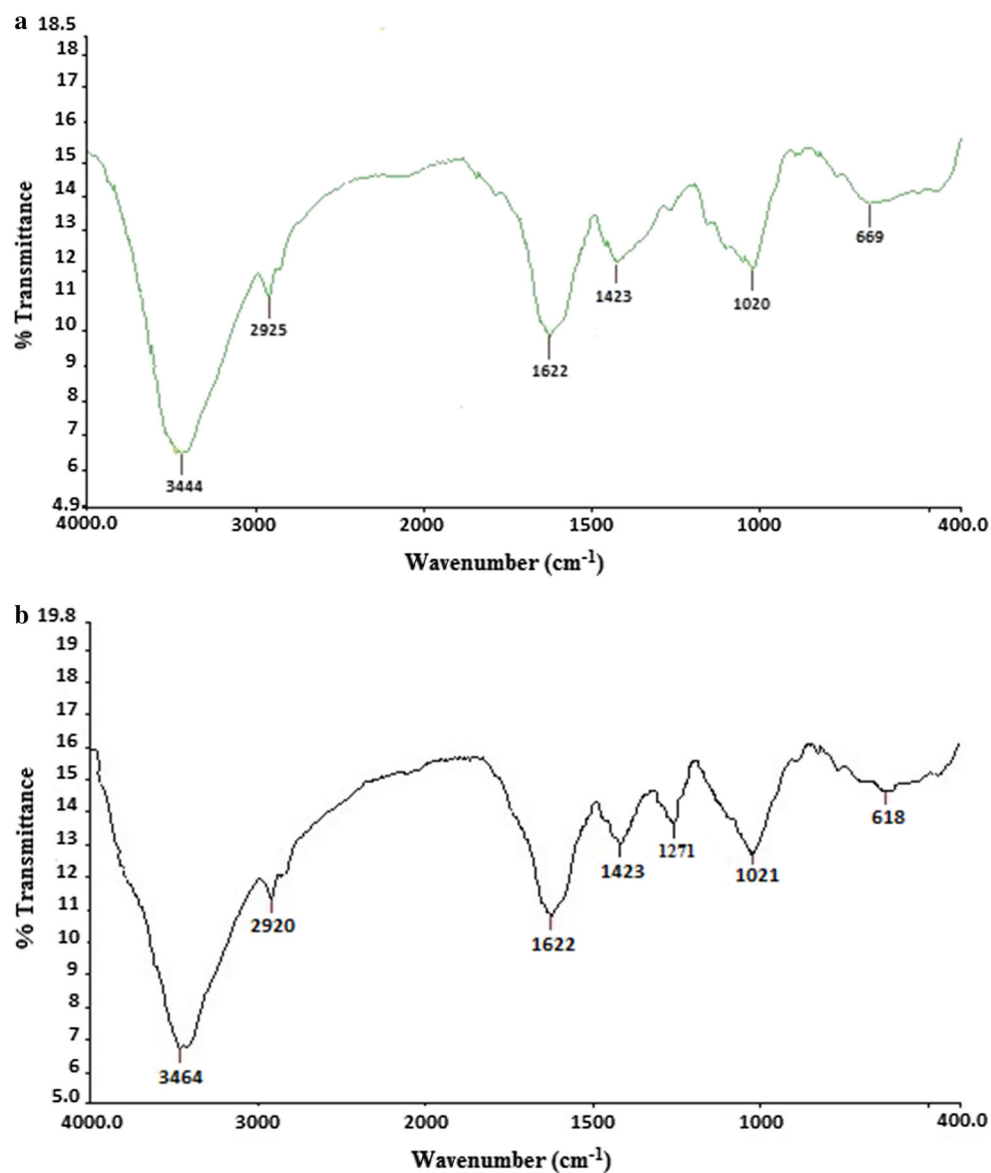


Fig. 1 Scanning electron microscopy images of NTFR biosorbent **a** before adsorption and **b** after adsorption of dye

Fig. 2 **a** FTIR spectra of NTFR before adsorption. **b** FTIR spectra of NTFR after adsorption



due to C=O stretching from the carboxylic group of biosorbent. The peak at 1423 cm^{-1} is attributed to the symmetric bending of CH_3 (Han et al. 2011; Kumar and Barakat 2013). The peak at 1020 cm^{-1} is due to stretch vibration of C–O–C in the lignin structure of the biosorbent. The peak at 1271 cm^{-1} observed after adsorption (Fig. 2b) is attributed to the C–N group interactions which could have occurred between C=O from carboxylic group of biosorbent and amine group ($-\text{NH}_2$) of the dye. From the FTIR analyses, it is established that carboxylic and hydroxyl groups of the NTFR biosorbent are mainly responsible for the adsorption of AB 25 dye. BET specific surface area, pore volume and average pore diameter were observed to be $136.26\text{ m}^2/\text{g}$, $0.021\text{ cm}^3/\text{g}$ and 6.12 nm , respectively. The average pore diameter established in the work confirmed the existence of mesoporous region of the NTFR pores.

Effect of pH

pH is the important factor influencing dye adsorption as the operating pH affects surface chemistry of the biosorbent. Experiments were conducted at different pH values of 2, 4, 6, 8 and 10 to study the influence on the extent of dye removal. The obtained results indicated a decrease in the extent of dye removal from 98.55 ± 0.79 to $32.24 \pm 0.67\%$ with an increase in the pH from 2 to 10 at otherwise similar operating conditions. At lower pH, cationic charge is developed on the biosorbent surface and hence anionic dye is adsorbed to a higher extent on the surface due to the electrostatic attractions (Safa and Bhatti 2011) leading to maximum AB 25 dye removal. Similar results have been reported for removal of Congo red dye using adsorbent obtained from cattail root (Hu et al. 2010), open burnt clay (Mumin et al. 2007) and activated carbon fibers obtained from silkworm cocoon waste (Li et al. 2015). The obtained results of maximum dye removal at lower pH are also confirmed based on the pH_{pzc} value of NTFR biosorbent (observed as 7.48 in the present work) as the cationic charge is developed on the biosorbent surface below pH of 7.48 leading to higher degree of anionic dye removal.

Effect of biosorbent dose (m)

The study related to the effect of biosorbent dose helps in determining the maximum capacity of biosorbent for the removal of given dye. The effect of biosorbent dosage on the removal of AB 25 by NTFR over the range from 1 to 10 g/L is depicted in Fig. 3. Dye removal was significantly increased from $50.94 \pm 1.37\%$ at 1 g/L to $98.55 \pm 0.85\%$ at 4 g/L loading for NTFR biosorbent. This rapid increase in the dye removal with an increase in the biosorbent dose is attributed to the availability of large surface area which makes more sites available for the adsorption (Nandi et al.

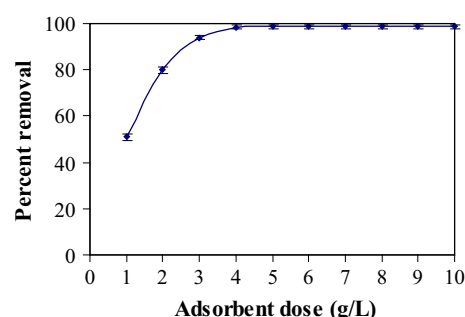


Fig. 3 Effect of biosorbent dose on the removal of AB 25 by NTFR biosorbent ($T = 303\text{ K}$, $t = 3\text{ h}$, $C_i = 100\text{ mg/L}$, $\text{pH}_i = 2$)

2009; Palizban 2016). The extent of removal slightly increased from 98.55 ± 0.85 to $98.73 \pm 0.83\%$ for a subsequent increase in the biosorbent loading from 4 to 10 g/L. Above the loading of 4 g/L, adsorption equilibrium of dye is quickly reached and hence removal of dye is only marginally affected for any higher biosorbent dosage of above 4 g/L. The observed optimum biosorbent dose of 4 g/L was used in the subsequent experiments. Similar trend has been reported for removal of basic dyes using biosorbent based on rice straw (Gong et al. 2008).

Effect of contact time (t)

The effect of contact time on the extent of AB 25 removal by NTFR biosorbent at different initial dye concentrations as 50, 100, 150 and 200 mg/L is shown in Fig. 4. It can be seen from the figure that rapid dye adsorption is obtained in first 30 min of treatment and thereafter, the rate of adsorption decreased gradually and equilibrium is reached in about 3 h. Further increase in contact time up to 5 h showed that the increase in dye removal was only about 0.2486% over those obtained for contact time of 3 h. Hence, 3 h has been considered as the equilibrium time and

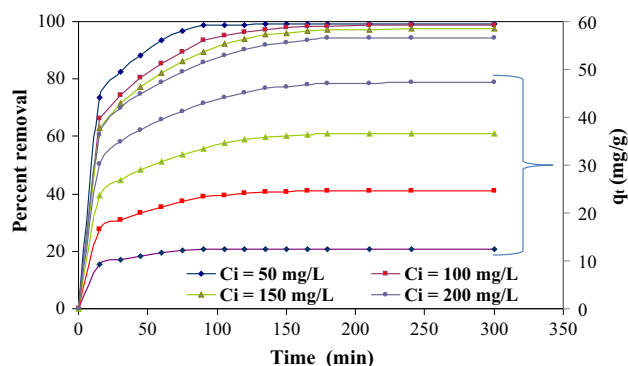


Fig. 4 Effect of contact time and initial dye concentration on the removal of AB 25 by NTFR biosorbent ($T = 303\text{ K}$, $t = 5\text{ h}$, $C_i = 50\text{--}200\text{ mg/L}$, $\text{pH}_i = 2$, $m = 4\text{ mg/L}$, the bottom four lines highlighted by curly bracket refers to q_t , whereas top four lines refer to the percent removal data)



all the batch adsorption experiments were performed for 3 h contact time. Similar trend has been reported for removal of brilliant green dye using biosorbent based on bagasse fly ash (Mane et al. 2007). Initially, a large number of vacant sites are available for dye adsorption, but with an increase in the treatment time, the remaining vacant sites are difficult to be occupied during later period of adsorption due to forces of repulsion between solute molecules on the adsorbent and bulk phases resulting in decreased adsorption rate (Ahmad and Alrozi 2011).

Effect of initial dye concentration (C_i)

The effect of C_i on the extent of dye removal is shown in Fig. 4. It is found that with an increase in C_i from 50 to 200 mg/L, q_t value increased from 12.4 ± 0.9 to 47.25 ± 0.6 mg/g. The increase in the q_t value can be attributed to the fact that an increase in the C_i increased the concentration driving force and hence the rate of external mass transfer increased, causing transfer of the dye from bulk solution to the surface of the adsorbent (Jalil et al. 2012). Similar trend has been reported for removal of AB 25 dye using biosorbent based on shrimp shell (Daneshvar et al. 2014) and brilliant green dye using biosorbent based on kaolin clay (Shirsath et al. 2013).

Adsorption kinetics

The adsorption mechanism is dependent on the physical and chemical characteristics of the adsorbent and the associated mass transfer processes (Ugurlu 2009). In the present study, adsorption kinetics of AB 25 onto biosorbent was investigated using three kinetic models.

Pseudo-first-order model

The governing equation for the pseudo-first-order model is expressed as follows (Lagergren 1898):

$$\frac{dq_t}{dt} = k_1(q_e - q_t) \quad (2)$$

where t is time (min), q_e is equilibrium adsorption capacity (mg/g), and k_1 is pseudo-first-order rate constant (min^{-1}). On integrating and applying the boundary conditions, the resulting equation is:

$$\ln(q_e - q_t) = -k_1 t + \ln q_e \quad (3)$$

The values of k_1 and $q_{e, \text{cal}}$ were calculated from the slope ($-k_1$) and intercept ($\ln q_e$) of the plot of $\ln(q_e - q_t)$ versus t , respectively, and the obtained values are depicted in Table 1. The correlation coefficient (R^2) values given in Table 1 are not significantly closer to unity, and also the $q_{e, \text{exp}}$ and $q_{e, \text{cal}}$ values are not close to each other, which

Table 1 Kinetic parameters for removal of AB 25 by NTFR biosorbent ($T = 303 \text{ K}$, $t = 5 \text{ h}$, $\text{pH}_i = 2$, $m = 4 \text{ mg/L}$)

Pseudo-first-order model				
C_i (mg/L)	$q_{e, \text{exp}}$ (mg/g)	$q_{e, \text{cal}}$ (mg/g)	k_1 (min^{-1})	R^2
50	12.39	4.87	0.0367	0.9478
100	24.7	21.03	0.0315	0.9876
150	36.6	29.31	0.0275	0.9869
200	47.25	40.78	0.0278	0.9740
Pseudo-second-order model				
C_i (mg/L)	$q_{e, \text{exp}}$ (mg/g)	$q_{e, \text{cal}}$ (mg/g)	k_2 ($\text{g mg}^{-1} \text{min}^{-1}$)	R^2
50	12.39	12.67	0.0175	0.9997
100	24.7	25.77	0.0039	0.9995
150	36.6	38.46	0.0021	0.9994
200	47.25	49.75	0.0016	0.9993
Weber–Morris intra-particle diffusion model				
C_i (mg/L)	k_{id} ($\text{mg g}^{-1} \text{min}^{-1/2}$)	I (mg/g)	Controlling step	R^2
50	0.61	6.91	Surface diffusion	0.9958
100	1.15	12.31	Surface diffusion	0.9952
150	1.64	17.77	Surface diffusion	0.9935
200	1.92	24.09	Surface diffusion	0.9813
50	0.0076	12.28	Pore diffusion	0.7141
100	0.085	23.36	Pore diffusion	0.6996
150	0.131	34.50	Pore diffusion	0.7011
200	0.142	44.95	Pore diffusion	0.6349

suggests that the adsorption kinetics did not follow pseudo-first-order model.

Pseudo-second-order model

The governing equation for the pseudo-second-order model is expressed as follows (Ho and McKay 1999):

$$\frac{dq_t}{dt} = k_2(q_e - q_t)^2 \quad (4)$$

where k_2 is pseudo-second-order rate constant ($\text{g mg}^{-1} \text{min}^{-1}$). On integrating and applying the boundary conditions, the resulting equation is:

$$\frac{t}{q_t} = \frac{t}{q_e} + \frac{1}{k_2 q_e^2} \quad (5)$$

The values of $q_{e, \text{cal}}$ and k_2 were calculated from the slope ($1/q_e$) and intercept ($1/k_2 q_e^2$) of the plot of t/q_t versus t , respectively, and the obtained values are given in Table 1. The correlation coefficient (R^2) values (average value 0.9995) given in Table 1 are very much closer to unity, and

$q_{e, \text{exp}}$ and $q_{e, \text{cal}}$ values are also close to each other for all the concentrations investigated in the work. These findings suggest that the adsorption kinetics is better represented by the pseudo-second-order model. Similar results have been reported for the removal of AB 25 by activated carbon (Tovar-gómez et al. 2014). The values of the pseudo-second-order rate constant (k_2) decreased from 0.0175 to 0.0016 g mg⁻¹ min⁻¹ as the initial concentration increased from 50 to 200 mg/L, showing that adsorption process is highly concentration dependent. Similar results have been reported for removal of crystal violet and methylene blue using adsorbent based on *Ferula orientalis* (Aysu and Kucuk 2015) and Astrazon Yellow 7GL using biosorbent based on wheat bran (Sulak et al. 2007). However, adsorption kinetics followed pseudo-first-order model for removal of AB 113 by commercial activated carbon and rubber tire based activated carbon (Gupta et al. 2011).

Intra-particle diffusion model

The Weber–Morris intra-particle diffusion model used in the present work can be mathematically expressed as follows (Weber and Carrell Morris 1963):

$$q_t = k_{id}t^{1/2} + I \quad (6)$$

where k_{id} is the intra-particle diffusion rate constant (mg g⁻¹ min^{-1/2}) and I is the model constant (mg/g). According to Eq. (6), if the plot of q_t versus $t^{1/2}$ is linear and not passing through the origin then the adsorption is limited by intra-particle diffusion and this is the rate-controlling step (Doğan et al. 2009). The obtained data in the present study did not yield a straight line with one constant slope (Fig. 5), indicating that intra-particle diffusion is not the sole rate-controlling step. It can be said that the adsorption of AB 25 on NTFR biosorbent is a multistep process. It can be also seen from the figure that there are two different straight line regions for all the concentrations investigated in the work. The first sharper line portion indicates surface adsorption or boundary layer diffusion is controlling, and second linear portion indicates intra-particle or pore diffusion is controlling (Nethaji et al. 2013). The fitting of two straight lines has thus confirmed that the rate-controlling step in the initial stages is surface diffusion, which shifts to the intra-particle diffusion in later stages as also reported in literature (Kumar and Kumaran 2005). Similar trend of multistep diffusion was reported for removal of AB 25 and Acid Red 337 using adsorbent derived from biomass of *Aspergillus oryzae* (Yang et al. 2011) and for the adsorption of direct blue 86 by activated carbon obtained from orange peel (Nemr et al. 2009).

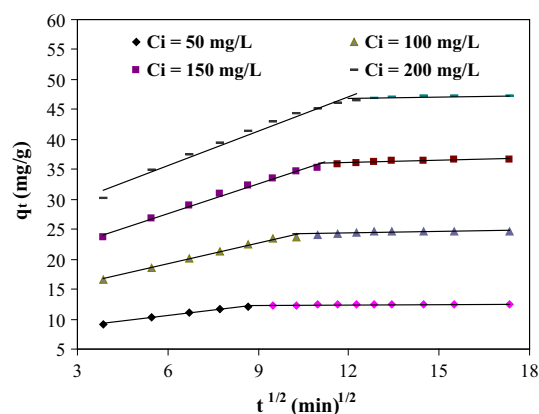


Fig. 5 Weber–Morris intra-particle diffusion plot for removal of AB 25 by NTFR biosorbent ($T = 303$ K, $t = 5$ h, $C_i = 50$ –200 mg/L, $\text{pH}_i = 2$, $m = 4$ mg/L)

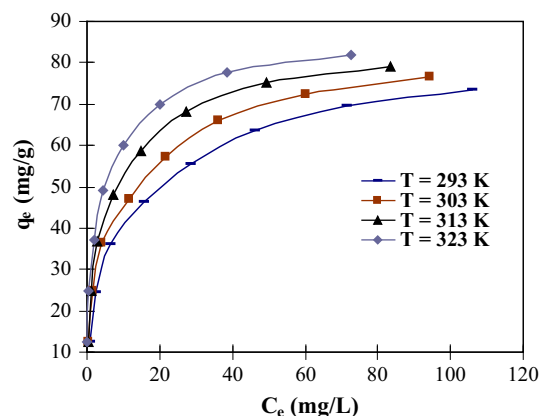


Fig. 6 Equilibrium adsorption isotherms at different temperatures for removal of AB 25 by NTFR biosorbent ($t = 3$ h, $C_i = 50$ –400 mg/L, $\text{pH}_i = 2$, $m = 4$ mg/L)

Effect of temperature

Figure 6 depicts the plot of equilibrium adsorption capacity, q_e , versus equilibrium dye concentration, C_e , at different temperatures of 293, 303, 313 and 323 K. The equilibrium adsorption capacity was found to increase with an increase in the temperature, indicating endothermic nature of the adsorption process (Kalavathy and Miranda 2010). The maximum adsorption capacity, q_m (mg/g), increased from 76.92 to 83.33 mg/g when temperature was increased from 293 to 323 K. Endothermic nature of the adsorption process is due to increase in mobility of the adsorbate and decrease in the retarding forces acting on diffusing adsorbate, with an increase in temperature. Similar results have been reported for removal of Congo red dye using biosorbent based on saw dust (Mane and Babu 2013). Exothermic nature was reported by earlier



researchers for the removal of AB 25 using biosorbent based on shrimp shell (Daneshvar et al. 2014) and base-treated *Shorea dasyphylla* sawdust based biosorbent (Hanafiah et al. 2012). Thus it is imperative to establish the dependency on temperature and the nature of adsorption process and the present work serves as a useful guideline.

Adsorption equilibrium study

Different isotherm equations are generally used to describe the adsorption equilibrium. In the present study, isotherm analysis was performed using Freundlich, Langmuir and Temkin adsorption isotherm equations. For better understanding, the model equations have been given now.

Freundlich isotherm model (Freundlich 1906) is expressed as follows:

$$q_e = K_F C_e^{1/n} \quad (7)$$

where K_F is Freundlich constant (mg/g)/(mg/L)^{1/n} indicating the adsorption capacity and $1/n$ is heterogeneous factor (dimensionless) indicating adsorption affinity. Langmuir isotherm model (Langmuir 1918) is expressed as follows:

$$q_e = \frac{q_m K_L C_e}{1 + K_L C_e} \quad (8)$$

where K_L is Langmuir constant (L/mg) indicating affinity of AB 25 dye to bind with the adsorbent and q_m is the maximum adsorption capacity (mg/g). Temkin isotherm model (Temkin and Pyzhev 1940) is expressed as follows:

$$q_e = B \ln(K_T C_e) \quad (9)$$

where B (mg/g) and K_T (L/mg) are Temkin constants. K_T indicates the adsorption affinity.

The obtained results for the linear fittings of these models are given in Table 2. It can be seen from the data reported in Table 2 that the correlation coefficient, R^2 , values (average value 0.9651) deviate from unity, indicating non-fitting of Freundlich isotherm to the experimental results obtained. On the other hand, correlation coefficient, R^2 , values (average value 0.9962) are much closer to unity, indicating better fitting of the Langmuir isotherm to the experimental results. The data given in Table 2 also show an increase in q_m and K_L with an increase in temperature, confirming endothermic nature of the adsorption process. For the Temkin model also, excellent fitting was observed as indicated by the values of the correlation coefficient, R^2 (average value 0.9925). The data presented in Table 2 also indicate that K_T for the Temkin model increased with an increase in temperature, also confirming endothermic nature of the adsorption process.

In addition to the correlation coefficient analysis, average relative error (ARE) analysis has also been employed

to check the best suitability of the isotherm model. The ARE function (Kapoor and Yang 1989) is given as follows:

$$ARE = \frac{100}{n} \sum_{i=1}^n \left| \frac{(q_{e,exp} - q_{e,calc})}{q_{e,exp}} \right|_i \quad (10)$$

where $q_{e,exp}$ is experimental value of q_e and $q_{e,calc}$ is the calculated value of q_e using the fitted model with n as the number of data points at a certain temperature. The obtained values of the ARE are given in Table 2 for the different fittings at different temperatures. ARE values were found to be the minimum for the Temkin model as compared to all the other isotherms confirming best results. The values of the correlation coefficient (R^2) were found to be the best for the Langmuir isotherm as compared to the other isotherms. Overall, it can be said that Langmuir and Temkin isotherms are found to best represent the data of adsorption of AB 25 on NTFR biosorbent.

Determination of thermodynamic parameters of adsorption

The thermodynamic parameters for the removal of AB 25 were quantified in terms of the values of change in Gibbs free energy, ΔG^0 (kJ/mol), change in enthalpy, ΔH^0 (kJ/mol), and change in entropy, ΔS^0 (kJ/mol K). Van't Hoff equation used for the estimation of these parameters is given as follows:

$$\Delta G^0 = -RT \ln K \quad (11)$$

where R is universal gas constant, T is absolute temperature (K), and K is equilibrium constant. Typically, ΔG^0 , ΔH^0 , ΔS^0 and T are related by the following equation:

$$\Delta G^0 = \Delta H^0 - T\Delta S^0 \quad (12)$$

By combining above two equations, we get

$$\ln K = -\frac{\Delta H^0}{R} \frac{1}{T} + \frac{\Delta S^0}{R} \quad (13)$$

The thermodynamic parameters are estimated from the plot of $\ln K$ versus $1/T$, and the obtained values are given in Table 2. ΔG^0 value has been observed to be negative, which confirms that adsorption is spontaneous (Ranjithkumar et al. 2014). This observed trend confirms the feasibility of the adsorption process. ΔG^0 increased with an increase in temperature from 293 to 323 K, indicating favorable adsorption with an increase in temperature. ΔH^0 is positive, indicating endothermic nature of the adsorption process (Srivastav and Srivastava 2009), whereas positive ΔS^0 confirmed increased randomness (Moussavi and Khosravi 2011) and affinity of FR biosorbent toward AB 25 dye (Önal et al. 2006).

Table 2 Isotherm and thermodynamic parameters for removal of AB 25 by NTFR biosorbent ($t = 3$ h, $C_i = 50$ – 400 mg/L, $pH_i = 2$, $m = 4$ mg/L)

Isotherm parameters						
Freundlich model: $q_e = K_F C_e^{1/n}$						
T (K)	K_F ((mg/g)/(mg/L) ^{1/n})	$1/n$	R^2	ARE		
293	16.68	0.345	0.9648	9.3761		
303	19.86	0.327	0.9645	9.7808		
313	23.81	0.307	0.9678	11.2882		
323	28.39	0.288	0.9634	10.6142		
Langmuir model: $q_e = \frac{q_m K_L C_e}{1 + K_L C_e}$						
T (K)	K_L (L/mg)	q_m (mg/g)	R^2	ARE		
293	0.134	76.92	0.9947	12.9353		
303	0.185	79.36	0.9954	15.3636		
313	0.275	81.30	0.9970	13.5264		
323	0.417	83.33	0.9978	17.9534		
Temkin model: $q_e = B \ln (K_T C_e)$						
T (K)	K_T (L/mg)	B (mg/g)	R^2	ARE		
293	3.15	12.54	0.9947	3.9388		
303	5.33	12.24	0.9936	4.5720		
313	10.13	11.77	0.9907	5.4370		
323	20.15	11.34	0.9910	6.4755		
Thermodynamic parameters at different temperatures						
Isotherm model	ΔG^0 (kJ/mol)				ΔH^0 (kJ/mol)	ΔS^0 (kJ/mol K)
	293 K	303 K	313 K	323 K		
Freundlich	−38.37	−40.12	−41.92	−43.73	13.97	0.178
Langmuir	−26.62	−28.34	−30.31	−32.4	29.85	0.192
Temkin	−34.32	−36.81	−39.7	−42.8	48.74	0.283

Comparison with other adsorbents

In order to have an idea of the effectiveness of NTFR as biosorbent for AB 25 dye removal from aqueous solution, the obtained maximum adsorption capacity has been compared with some of the adsorbents whose q_m values have been reported in the literature for removal of different anionic dyes (Table 3). It can be seen from these data that synthesized NTFR biosorbent in present study has comparatively good q_m value, 83.33 mg/g. From Table 3, it can be seen that q_m value of NTFR biosorbent is comparatively higher than the adsorption capacity of different adsorbents reported in the literature. Hence, it is reasonable to suggest that synthesized NTFR biosorbent in the present study is an efficient biosorbent for AB 25 removal from aqueous solution.

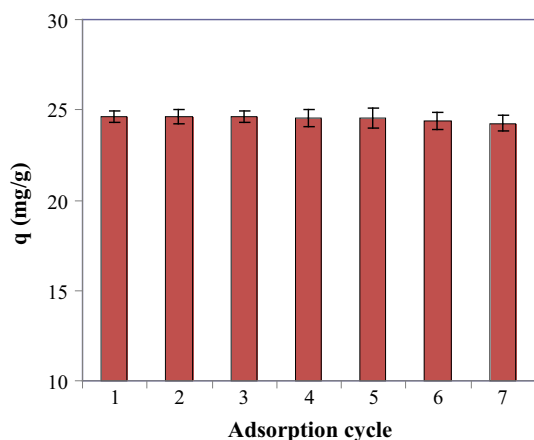
Reusability studies

The potential of the biosorbent depends on its repeated use, which also decides the economical feasibility of the treatment process. Reusability of NTFR biosorbent was determined by conducting adsorption–desorption process of 100 mg/L of AB 25 dye solution for seven cycles. Desorption process was performed by shaking dye-loaded NTFR biosorbent in the presence of distilled water at pH of 12. The biosorption process of AB 25 dye is favored at lower pH, whereas desorption is favored at higher pH. At pH 12, high electrostatic interaction exists between anionic dye-loaded biosorbent and alkaline distilled water, which resulted in fast desorption of dye from NTFR biosorbent. The obtained adsorption capacities, q (mg/g), in each cycle are presented in Fig. 7. The adsorption capacity was



Table 3 Maximum adsorption capacity (q_m) for removal of various anionic dyes from aqueous solution using different biomass based adsorbents

Anionic dyes	Biomass used for obtaining Adsorbents	q_m (mg/g)	pH	Temperature	References
AB 25	NaOH-treated FR (NTFR)	83.33	2	323	Present study
AB 25	<i>Shorea dasyphylla</i> sawdust treated with alkali	24.39	2	300	Hanafiah et al. (2012)
AB 25	Hazelnut shell	60.2	2.5	293	Ferrero (2007)
Congo red	NaOH-treated saw dust	66.67	7	318	Mane and Babu (2013)
Congo red	Jujuba seeds	55.56	2	333	Reddy et al. (2012)
Congo red	Jute stick powder	35.7	7	303	Panda et al. (2009)
Congo red	Phoenix dactylifera seeds	61.72	2	333	Pathania et al. (2016)
Remazol red B	Thermally activated sepiolite	9.44	2	313	Ugurlu (2009)
Remazol red B	Acid-activated sepiolite	9.94	2	313	Ugurlu (2009)
AB 113	Commercial activated carbon	7.84	5	298	Gupta et al. (2011)
AB 113	Rubber tire activated carbon	9.72	2	298	Gupta et al. (2011)
Direct blue 86	Activated carbon from orange peel	33.78	2	298	Nemr et al. (2009)
Acid yellow 17	Activated carbon/ α -Fe ₂ O ₃ nanocomposite	71.43	1	323	Ranjithkumar et al. (2014)
Indosol Yellow BG	Acetic acid-treated peanut husk biomass	79.7	2	303	Sadaf and Bhatti (2014)
Acid orange 10	Activated carbon prepared from sugarcane bagasse	5.78	2.3	313	Tsai et al. (2001)

**Fig. 7** Reusability studies of NTFR biosorbent for seven cycles

observed to be slightly decreased from 24.64 ± 0.34 mg/g for first cycle to 24.36 ± 0.42 mg/g for the seventh cycle. The obtained results showed that NTFR biosorbent could be regenerated and used repeatedly for the treatment. Hence, the synthesized NTFR biosorbent in present study is an efficient biosorbent to remove AB 25 dye, which ensures its potential and applicability to treat dye effluents.

Conclusion

The present study has clearly established the fact that NaOH-treated FR dead leaves (NTFR) can be used as an effective biosorbent for the removal of AB 25 from aqueous solution. The extent of the dye removal was found to

vary with pH, biosorbent dose, contact time, initial concentration and temperature. Dye removal was found to decrease with an increase in pH, and optimum pH of 2 was reported. The equilibrium time established in the work was 3 h. The study related to the effect of operating parameters revealed that the adsorption capacity was significantly increased with an increase in the concentration and temperature. The extent of dye removal was found to be almost 100% for 100 mg/L of initial dye concentration in a contact time of 3 h at 323 K, indicating efficiency of the biosorbent for dye removal. The adsorption kinetics followed pseudo-second-order model. Kinetic study also confirmed that adsorption is a multistep process consisting of rate controlling steps as surface diffusion followed by intra-particle diffusion. Langmuir and Temkin isotherms were found to provide the best fit to the experimental data. The maximum adsorption capacity was observed to be 83.33 mg/g. Repeated use of the biosorbents for seven cycles also confirmed reusability of synthesized NTFR biosorbent. Overall, it has been established that the NaOH-treated FR dead leaves serve as a low-cost, effective biosorbent and can be considered as promising biosorbent to remove AB 25 from wastewater.

Acknowledgements The authors gratefully acknowledge University Grants Commission for assistance under UGC-NRC, at the Institute of Chemical Technology, Mumbai, Maharashtra, India.

References

- Ahmad MA, Alrozi R (2011) Removal of malachite green dye from aqueous solution using rambutan peel-based activated carbon:



- equilibrium, kinetic and thermodynamic studies. *Chem Eng J* 171:510–516
- Aksu Z, Tatli AI, Tunç Ö (2008) A comparative adsorption/biosorption study of Acid Blue 161: effect of temperature on equilibrium and kinetic parameters. *Chem Eng J* 142:23–39
- Angin D (2014) Utilization of activated carbon produced from fruit juice industry solid waste for the adsorption of yellow 18 from aqueous solutions. *Bioresour Technol* 168:259–266
- Aysu T, Kucuk MM (2015) Removal of crystal violet and methylene blue from aqueous solutions by activated carbon prepared from *Ferula orientalis*. *Int J Environ Sci Technol* 12:2273–2284
- Benadjemia M, Millièrè L, Reinert L et al (2011) Preparation, characterization and methylene blue adsorption of phosphoric acid activated carbons from globe artichoke leaves. *Fuel Process Technol* 92:1203–1212
- Daneshvar E, Salar M, Kousha M et al (2014) Shrimp shell as an efficient bioadsorbent for Acid Blue 25 dye removal from aqueous solution. *J Taiwan Inst Chem Eng* 45:2926–2934
- Doğan M, Abak H, Alkan M (2009) Adsorption of methylene blue onto hazelnut shell: kinetics, mechanism and activation parameters. *J Hazard Mater* 164:172–181
- Duman O, Tunç S, Kancı B (2011) Spectrophotometric studies on the interactions of C.I. Basic Red 9 and C.I. Acid Blue 25 with hexadecyltrimethylammonium bromide in cationic surfactant micelles. *Fluid Phase Equilib* 301:56–61
- El NA, Abdelwahab O, El-Sikaily A, Khaled A (2009) Removal of direct blue-86 from aqueous solution by new activated carbon developed from orange peel. *J Hazard Mater* 161:102–110
- Ferrero F (2007) Dye removal by low cost adsorbents: hazelnut shells in comparison with wood sawdust. *J Hazard Mater* 142:144–152
- Freundlich HMF (1906) Over the adsorption in solution. *J Phys Chem* 57:385–470
- Gong R, Jin Y, Sun J, Zhong K (2008) Preparation and utilization of rice straw bearing carboxyl groups for removal of basic dyes from aqueous solution. *Dye Pigment* 76:519–524
- Greluk M, Hubicki Z (2011) Efficient removal of Acid Orange 7 dye from water using the strongly basic anion exchange resin Amberlite IRA-958. *Desalination* 278:219–226
- Gupta VK, Suhas (2009) Application of low-cost adsorbents for dye removal—a review. *J Environ Manag* 90:2313–2342
- Gupta VK, Gupta B, Rastogi A et al (2011) A comparative investigation on adsorption performances of mesoporous activated carbon prepared from waste rubber tire and activated carbon for a hazardous azo dye—Acid Blue 113. *J Hazard Mater* 186:891–901
- Han R, Wang Y, Zhao X et al (2009) Adsorption of methylene blue by phoenix tree leaf powder in a fixed-bed column: experiments and prediction of breakthrough curves. *Desalination* 245:284–297
- Han X, Wang W, Ma X (2011) Adsorption characteristics of methylene blue onto low cost biomass material lotus leaf. *Chem Eng J* 171:1–8
- Hanafiah MAKM, Ngah WSW, Zolkafly SH et al (2012) Acid Blue 25 adsorption on base treated *Shorea dasyphylla* sawdust: kinetic, isotherm, thermodynamic and spectroscopic analysis. *J Environ Sci* 24:261–268
- Ho YS, McKay G (1999) Pseudo-second order model for sorption processes. *Process Biochem* 34:451–465
- Hu Z, Chen H, Ji F, Yuan S (2010) Removal of Congo Red from aqueous solution by cattail root. *J Hazard Mater* 173:292–297
- Jalil AA, Triwahyono S, Yaakob MR et al (2012) Utilization of bivalve shell-treated *Zea mays* L. (maize) husk leaf as a low-cost biosorbent for enhanced adsorption of malachite green. *Bioresour Technol* 120:218–224
- Janoš P, Michálek P, Turek L (2007) Sorption of ionic dyes onto untreated low-rank coal—oxihumolite: a kinetic study. *Dye Pigment* 74:363–370
- Kalavathy MH, Miranda LR (2010) Comparison of copper adsorption from aqueous solution using modified and unmodified *Hevea brasiliensis* saw dust. *Desalination* 255:165–174
- Kapoor A, Yang RT (1989) Correlation of equilibrium adsorption data of condensable vapours on porous adsorbents. *Gas Sep Purif* 3:187–192
- Kumar R, Barakat MA (2013) Decolourization of hazardous brilliant green from aqueous solution using binary oxidized cactus fruit peel. *Chem Eng J* 226:377–383
- Kumar KV, Kumaran A (2005) Removal of methylene blue by mango seed kernel powder. *Biochem Eng J* 27:83–93
- Kumar PS, Ramalingam S, Senthamarai C et al (2010) Adsorption of dye from aqueous solution by cashew nut shell: studies on equilibrium isotherm, kinetics and thermodynamics of interactions. *Desalination* 261:52–60
- Lagergren S (1898) About the theory of so called adsorption of soluble substances. *Ksver Vetenskapsakad Handl* 24:1–6
- Langmuir I (1918) The adsorption of gases on plane surfaces of glass, mica and platinum. *J Am Chem Soc* 40:1361–1403
- Lee LY, Chin DZB, Lee XJ et al (2014) Evaluation of *Abelmoschus esculentus* (lady's finger) seed as a novel biosorbent for the removal of Acid Blue 113 dye from aqueous solutions. *Process Saf Environ Protoc* 94:329–338
- Li J, Ng DHL, Song P et al (2015) Preparation and characterization of high-surface-area activated carbon fibers from silkworm cocoon waste for congo red adsorption. *Biomass Bioenergy* 75:189–200
- Lin L, Zhai S-R, Xiao Z-Y et al (2013) Dye adsorption of mesoporous activated carbons produced from NaOH-pretreated rice husks. *Bioresour Technol* 136:437–443
- Malik PK, Saha SK (2003) Oxidation of direct dyes with hydrogen peroxide using ferrous ion as catalyst. *Sep Purif Technol* 31:241–250
- Mane VS, Babu PVV (2013) Kinetic and equilibrium studies on the removal of Congo red from aqueous solution using Eucalyptus wood (*Eucalyptus globulus*) saw dust. *J Taiwan Inst Chem Eng* 44:81–88
- Mane VS, Mall ID, Srivastava VC (2007) Use of bagasse fly ash as an adsorbent for the removal of brilliant green dye from aqueous solution. *Dye Pigment* 73:269–278
- Mokri HSG, Modirshahla N, Behnajady MA, Vahid B (2015) Adsorption of C.I. Acid Red 97 dye from aqueous solution onto walnut shell: kinetics, thermodynamics parameters, isotherms. *Int J Environ Sci Technol* 12:1401–1408
- Moussavi G, Khosravi R (2011) The removal of cationic dyes from aqueous solutions by adsorption onto pistachio hull waste. *Chem Eng Res Des* 89:2182–2189
- Mumin MA, Khan MMR, Akhter KF, Uddin MJ (2007) Potentiality of open burnt clay as an adsorbent for the removal of Congo red from aqueous solution. *Int J Environ Sci Technol* 4:525–532
- Muneer M, Adeel S, Bhatti IA et al (2015) Removal of reactive orange P3R dye by oxidative pathway. *Oxid Commun* 38:808–817
- Nandi BK, Goswami A, Purkait MK (2009) Adsorption characteristics of brilliant green dye on kaolin. *J Hazard Mater* 161:387–395
- Nethaji S, Sivasamy A, Mandal AB (2013) Adsorption isotherms, kinetics and mechanism for the adsorption of cationic and anionic dyes onto carbonaceous particles prepared from *Juglans regia* shell biomass. *Int J Environ Sci Technol* 10:231–242
- Önal Y, Akmil-Başar C, Eren D et al (2006) Adsorption kinetics of malachite green onto activated carbon prepared from Tunçbilek lignite. *J Hazard Mater* 128:150–157
- Palizban EGZ (2016) Comparisons of azo dye adsorptions onto activated carbon and silicon carbide nanoparticles loaded on activated carbon. *Int J Environ Sci Technol* 13:501–512



- Panda GC, Das SK, Guha AK (2009) Jute stick powder as a potential biomass for the removal of congo red and rhodamine B from their aqueous solution. *J Hazard Mater* 164:374–379
- Pathania D, Sharma A, Siddiqi Z (2016) Removal of congo red dye from aqueous system using *Phoenix dactylifera* seeds. *J Mol Liq* 219:359–367
- Pavan FA, Camacho ES, Lima EC et al (2014) Formosa papaya seed powder (FPSP): preparation, characterization and application as an alternative adsorbent for the removal of crystal violet from aqueous phase. *J Environ Chem Eng* 2:230–238
- Peydayesh M, Rahbar-Kelishami A (2015) Adsorption of methylene blue onto *Platanus orientalis* leaf powder: kinetic, equilibrium and thermodynamic studies. *J Ind Eng Chem* 21:1014–1019
- Ranjithkumar V, Sangeetha S, Vairam S (2014) Synthesis of magnetic activated carbon/ α -Fe₂O₃ nanocomposite and its application in the removal of acid yellow 17 dye from water. *J Hazard Mater* 273:127–135
- Reddy MCS, Sivaramakrishna L, Reddy AV (2012) The use of an agricultural waste material, Jujuba seeds for the removal of anionic dye (Congo red) from aqueous medium. *J Hazard Mater* 203–204:118–127
- Sachdeva S, Kumar A (2009) Preparation of nanoporous composite carbon membrane for separation of rhodamine B dye. *J Memb Sci* 329:2–10
- Sadaf S, Bhatti HN (2014) Batch and fixed bed column studies for the removal of Indosol Yellow BG dye by peanut husk. *J Taiwan Inst Chem Eng* 45:541–553
- Saeed A, Sharif M, Iqbal M (2010) Application potential of grapefruit peel as dye sorbent: kinetics, equilibrium and mechanism of crystal violet adsorption. *J Hazard Mater* 179:564–572
- Saeed M, Adeel S, Ilyas M et al (2015a) Oxidative degradation of methyl orange catalyzed by lab prepared nickel hydroxide in aqueous medium. *Desalin Water Treat* 57:1–10
- Saeed M, Adeel S, Shahzad MA et al (2015b) Pt/Al₂O₃ catalyzed decolorization of Rhodamine B dye in aqueous medium. *Chiang Mai J Sci* 42:730–744
- Saeed M, Haq A, Muneer M et al (2016) Degradation of direct black 38 dye catalyzed by lab prepared nickel hydroxide in aqueous medium. *Glob Nest* 18:309–320
- Safa Y, Bhatti HN (2011) Adsorptive removal of direct textile dyes by low cost agricultural waste: application of factorial design analysis. *Chem Eng J* 167:35–41
- Saygılı H, Güzel F (2015) Performance of new mesoporous carbon sorbent prepared from grape industrial processing wastes for malachite green and congo red removal. *Chem Eng Res Des* 100:27–38
- Shi B, Li G, Wang D et al (2007) Removal of direct dyes by coagulation: the performance of preformed polymeric aluminum species. *J Hazard Mater* 143:567–574
- Shirsath SR, Patil AP, Patil R et al (2013) Removal of brilliant green from wastewater using conventional and ultrasonically prepared poly (acrylic acid) hydrogel loaded with kaolin clay: a comparative study. *Ultrason Sonochem* 20:914–923
- Srivastav A, Srivastava VC (2009) Adsorptive desulfurization by activated alumina. *J Hazard Mater* 170:1133–1140
- Sulak MT, Demirbas E, Kobya M (2007) Removal of astrazon yellow 7GL from aqueous solutions by adsorption onto wheat bran. *Bioresour Technol* 98:2590–2598
- Temkin MJ, Pyzhev V (1940) Recent modifications to Langmuir isotherms. *Acta Physicochim USSR* 12:217–225
- Toor M, Jin B, Dai S, Vimonses V (2015) Activating natural bentonite as a cost-effective adsorbent for removal of Congo-red in wastewater. *J Ind Eng Chem* 21:653–661
- Tovar-Gómez R, Rivera-Ramírez DA, Hernández-Montoya V et al (2012) Synergic adsorption in the simultaneous removal of Acid Blue 25 and heavy metals from water using a Ca(PO₃)₂-modified carbon. *J Hazard Mater* 199–200:290–300
- Tovar-gómez R, Moreno-virgen R, Moreno-pérez J et al (2014) Analysis of synergistic and antagonistic adsorption of heavy metals and Acid Blue 25 on activated carbon from ternary systems. *Chem Eng Res Des* 93:755–772
- Tsai WT, Chang CY, Lin MC et al (2001) Adsorption of acid dye onto activated carbons prepared from agricultural waste bagasse by ZnCl₂ activation. *Chemosphere* 45:51–58
- Ugurlu M (2009) Adsorption of a textile dye onto activated sepiolite. *Microporous Mesoporous Mater* 119:276–283
- Unuabonah EI, Adie GU, Onah LO, Adeyemi OG (2009) Multistage optimization of the adsorption of methylene blue dye onto defatted *Carica papaya* seeds. *Chem Eng J* 155:567–579
- Weber WJ, Carrell Morris J (1963) Kinetics of adsorption on carbon from solution. *J Sanit Eng Div Am Soc Civ Eng* 89:31–60
- Yagub MT, Sen TK, Afroze S, Ang HM (2014) Dye and its removal from aqueous solution by adsorption: a review. *Adv Colloid Interface Sci* 209:172–184
- Yang Y, Jin D, Wang G et al (2011) Competitive biosorption of Acid Blue 25 and Acid Red 337 onto unmodified and CDAB-modified biomass of *Aspergillus oryzae*. *Bioresour Technol* 102:7429–7436
- Zhao B, Shang Y, Xiao W et al (2014) Adsorption of Congo red from solution using cationic surfactant modified wheat straw in column model. *J Environ Chem Eng* 2:40–45

